Korean J. Chem. Eng., **29**(3), 392-395 (2012)
DOI: 10.1007/s11814-011-0181-7

Mathematical analysis of colonial formation of embryonic stem cells in microfluidic system

Seul Ki Min*,‡, Byung Man Lee*,‡, Jin Ha Hwang*, Sung Ho Ha, and Hwa Sung Shin*,†**

*Department of Biological Engineering, Inha University, Incheon 402-751, Korea
**Departmet of Chemical Engineering & Nano-Bio Technology, Hannam University, Daejeon 305-811, Korea
(*Received 27 May 2011 • accepted 15 July 2011*)

Abstract−A fluidic environment affects mechanochemical characteristics of embryonic stem cells (ESCs). Perfusion is recognized as an attractive culture mode of ESCs since the steady fluidic state can enhance ESCs' controllability, supporting a unique cell culture condition. Cellular membrane motility presents important information about cellular dynamics such as adhesion, spreading, and migration. Thus, an investigation of the perfusion-induced membrane motility is significant to understand the mechanochemical behavior of ESCs in the steady culture state. In this research, we suggest L_{fr}, the ratio of circumferential membrane unattached to other cells' to the cell's circumference, as a new parameter to characterize cells' shape and motility. L_{fr} of embryonic stem cells has positive correlations with cellular area (A_r) and free peripheral length (L_f) but a negative correlation with roundness (R_n). We also propose a mathematical model representing ESCs' membrane motilities and demonstrate their colonical behavior.

Key words: Embryonic Stem Cells, Morphology, Self-renewal, Perfusion Culture, Free Peripheral Length Ratio (L_{fr})

INTRODUCTION

Embryonic stem cells (ESCs) derived from the inner cell mass of blastocysts can be both proliferated unlimitedly and differentiated into all lineages of cells [1]. This self-renewal and differentiation potency of ESCs has made them to be cell therapy sources for regenerative medicines [2]. With increasing interest in therapeutic applications of ESCs, more concerns and considerations to understand working mechanisms of the ESCs have been evoked with respect to safety and efficacy.

Perfusion culture is a promising method for maintaining or propagating ESCs [3] in that they are exposed to a continuous and steady fluidics, which is a favorable environment to control. However, under fluidic conditions, many types of cells alter their shapes and functions in response to mechanical forces such as shear stress and stretching tension [4]. Early researches reported cell elongation is affected by the fluidic flow direction [5] and also demonstrated shear stress can control gene expression related to inflammation [5], thrombosis [6], cell growth [7] and angiogenesis [8]. Shear stress has been known to affect ESC self-renewal, differentiation and intracellular genetic expression patterns. For example, fluidic direction that acts on node of mouse embryos brings out left-right asymmetry in the body completion [9], and shear stress induces genetic changes of differentiation and formation of tube-like structure [10].

Adhesion plays a critical role in cellular behavior and its significance to ESCs' fate is widely recognized. Shear stress under perfusion condition influences cellular adhesion mechanisms and intracellular signaling pathways. Adhesion status is reflected by morphological behavior, and thus its characterization is pivotal for analyzing cellular dynamic behavior. Therefore, morphological analysis of ESCs under a shear stress can give insights to understand ESCs' fate in perfusion culture mode.

In this study, we focused on analyzing morphological characteristics of outermost cells centered on mouse ESC's colonies exposed to microfluidic shear stress. The outermost cells have a part of the membrane which is not attached to any other cells but is just exposed to fluidic space. L_f, free peripheral length, is proposed to be a new index for analyzing cells' shape and motility along with its fraction, L_{fr}, ratio of free peripheral length. Finally, with the help of these indices, we proposed an analytical model to represent outermost cells' membrane behavior and mathematically discussed how ESCs grow in a colonial form.

MATERIALS AND METHODS

1. Microfluidic Device Fabrication

The microfluidic device was fabricated by soft lithography using PDMS (polydimethylsiloxane) [11,12]. Device pattern was designed purposefully using CAD program. The microfluidic device is composed of three channels and reservoirs, one outlet port, and culture chamber shown in Fig. 1. Each channel and reservoir has 20 μm width and 100 μm radius, respectively. The culture chamber is 500 μm wide. SU-8 negative PR (photoresist) was used to make a master pattern as 100-μm, against which PDMS was molded to get a PDMS replica. A PDMS punch was used to make reservoirs and outlet port.

2. Mouse ESCs Culture

E14 complete medium containing 500 ml Glasgow Minimum Essential Medium (G-MEM, Sigma, USA), 57 ml ES-cell certified FBS (HyClone, USA), 5.7 ml 200 mM L-glutamine, 5.7 ml 100 mM sodium pyruvates (Invitrogen, USA), 5.7 ml MEM Non-Essential Amino Acids Soln (Invitrogen, USA), 0.57 ml, 1,000× β-ME Soln, and 0.06 *l* murine leukemia inhibitor factor (LIF) (Chemicon

†To whom correspondence should be addressed.
E-mail: hsshin@inha.ac.kr
‡Equally contributing authors

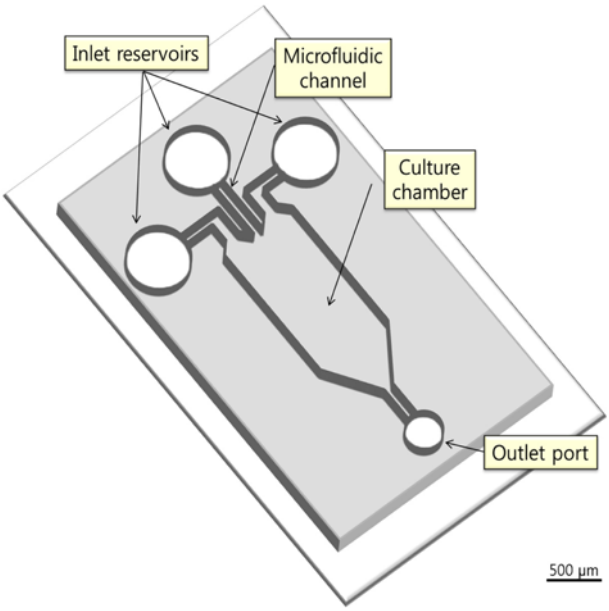

Fig. 1. Schematic design of microfluidic device for ESCs culture. The microfluidic device consists of the cell culture chamber, four channels and reservoirs. Cell culture media in the three inlet reservoirs is withdrawn out of the outlet part by microsyringe pump with 0.5 μl/min.

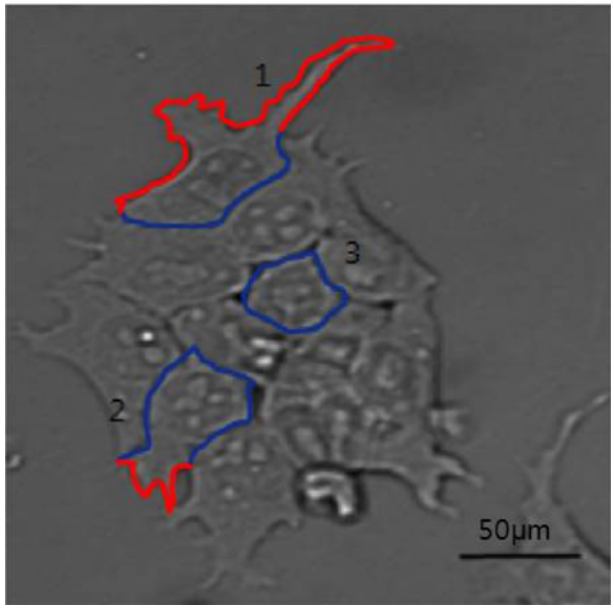

Fig. 2. A typical form of a cell cluster in the microfluidic device. The cells (number 1, 2 and 3) are typical examples showing each dissimilar cell-cell environment and membrane morphology. Red and blue lines each indicate L_f and L_{fix}.

International, USA) [13] was used for successful ESCs culture in 0.1% gelatin-coated dishes. Media was continuously changed in microfluidic device at 0.5 μl/min flow rate by a microsyringe pump. When cells reached 70-80% confluence, supernatant was eliminated and rinsed once with fresh E14 medium. Whenever the cells reached more than 90% confluence, the cells were passaged. All of the cell culture processes were maintained at 37 °C in a 5% CO_2 incubator.

3. Statistical Morphology Analysis

Each time-lapse image of cell clumps was captured every 30 minutes by a charge-coupled device (CCD) camera attached to an inverted microscopy (MICROS, Austria). Cell area (A_r), peripheral length (L_p) and free peripheral length (L_f) of randomly chosen three hundred cell images were measured each by means of 'INFINITY ANALYZE', an image analysis software (Lumenera corp., Canada). The cells completely isolated from or enclosed by surrounding cells, which each have 1 or 0 value of L_{fr}, were excepted from the subjects of the analyses. Correlation between L_{fr} and the set of A_r, L_{fr} and R_n were demonstrated by using statistical program (Minitab v15) with confidence level of P-value <0.05.

R_n/L_{fr} against L_{fr} and L_f was each correlated by nonlinear regression analysis, and the fitted curves with 95% coefficient of determination (R^2) were obtained using an inverse first-order equation Eq. (1) as follows:

$$\mathbf{f} = \mathbf{y}_0 + \frac{\mathbf{a}}{\mathbf{x}} \tag{1}$$

RESULTS AND DISCUSSION

1. Novel Characteristic Indices of Cellular Dynamic Morphology

Cell area A_r and peripheral length L_p are typical indices to characterize the cellular morphology, and the dimensionless index, roundness R_n, is formulated by them as published previously [14],

$$\mathbf{R}_n = \frac{4\pi \mathbf{A}_r}{\mathbf{L}_p^2} \tag{2}$$

Cells live as a form of either segregated single cells or a group, and in many cases they directly contact with surrounding cells by several reasons such as propagation, cell-cell interaction, cell-fusion, etc. These cells' activities make several variations in membrane morphology, influencing cellular A_r, L_p and R_n. For example, the cells numbered from 1 to 3 shown in Fig. 2, which are each in different cell to cell interaction condition, each show dissimilar morphological behavior. The peripheral membrane motilities are different between cells living alone and those directly contacting the other cells.

Free membrane regions (red lines of number 1 and 2 cells in Fig. 2) which directly contact to the fluidic environment show more heterogeneous motilities and thus L_f and its dimensionless value L_{fr} influence cellular A_r and R_n. Introducing L_f and L_{fr} as new indices, L_p can be replaced with L_f/L_{fr} and Eq. (2) is resultantly reformulated to Eq. (3), where L_{fr} has mathematical correlation with A_r, L_f and R_n.

$$\mathbf{R}_n = \frac{4\pi \mathbf{A}_r}{(\mathbf{L}_f/\mathbf{L}_{fr})^2} \tag{3}$$

To verify the efficacy of L_{fr} as a novel dimensionless number, it must first be proven to have correlations with independent variables, A_r, L_f and R_n. Following the image analysis procedure as mentioned above, A_r, L_f and R_n of each sampled cell were calculated and correlated with L_{fr} (Fig. 3).

Fig. 3 shows a negative correlation of R_n with L_{fr}, yielding - 0.698 Pearson correlation value. Active pseudopodia induces heterogeneous cell membrane motility, resulting in lower R_n as L_{fr} increases.

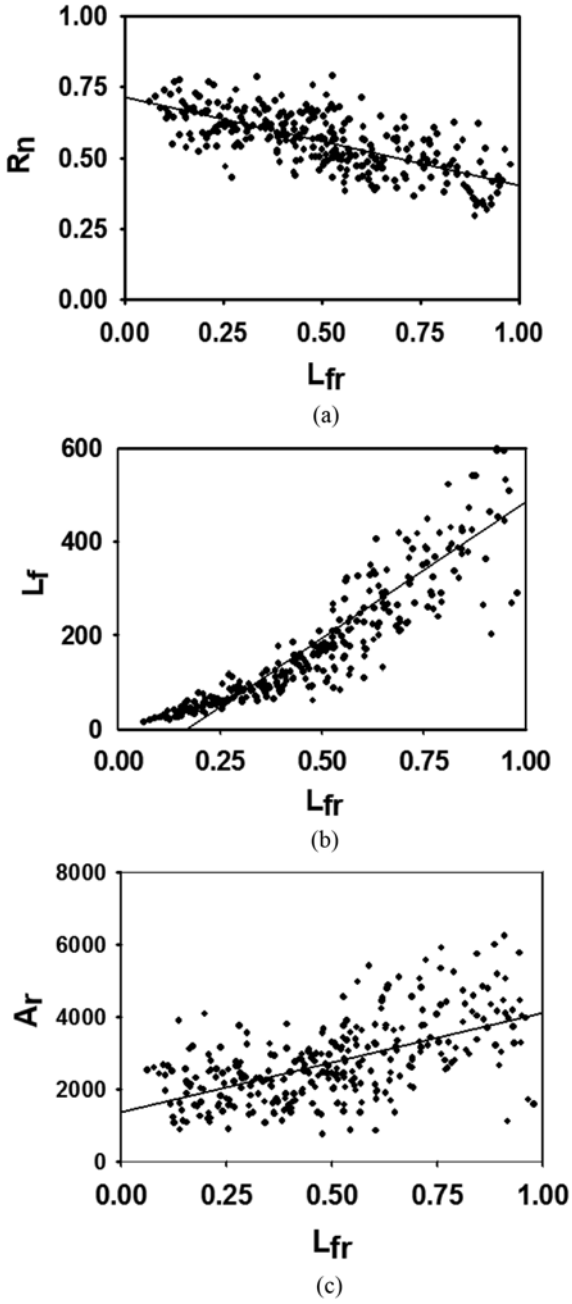

Fig. 3. Correlation figures of three parameters R_n (a), L_f (b) and A_r (c) with L_{fr}. L_{fr} of embryonic stem cells has positive correlations with A_r and L_f but a negative correlation with R_n. The vertical axis units of Fig. 3(b) and (c) are μm.

However, A_r proves to have a positive correlation with L_{fr}, and the positive 0.580 Pearson correlation value indicates that cells spread out much further when the peripheral membrane portion increases. Moreover, L_{fr} cannot help to increase with the increase of L_f as shown in Fig. 3, since a cell's L_p has an upper limit. In summary, even with certainty of standard deviation, Fig. 3 and the Pearson correlation test demonstrate that L_{fr} has correlations with independent variables, A_r, L_f and R_n.

2. Modeling of Morphological Variation in View of L_{fr} and L_f

Dimensionless number plays an important role in characterizing its corresponding system. Looking over Eq. (3), three independent variables, R_n, L_f, and L_{fr}, are used to represent cellular morphology. They can be re-formed to be R_n/L_{fr}, L_f, and L_{fr}, yielding one dimensionless number R_n/L_{fr}. The dimensionless number R_n/L_{fr} shows inverse correlations with L_f and L_{fr} as presented in Fig. 4.

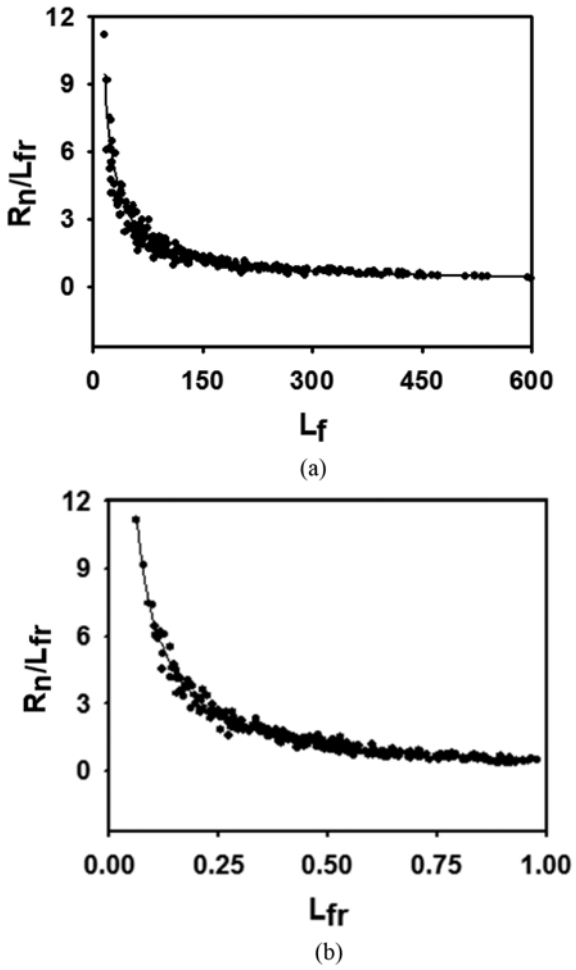

Fig. 4. Correlation figures of a dimensionless number R_n/L_{fr} with L_f (a) and L_{fr} (b).

We suggest regression models for their correlations as seen in Eq. (4) and (5), where a, b, c, and d are unknown parameters to be determined by regression analysis.

$$\frac{R_n}{L_{fr}} = a + \frac{b}{L_f} \tag{4}$$

$$\frac{R_n}{L_{fr}} = c + \frac{d}{L_{fr}} \tag{5}$$

Combining Eq. (4) and (5) gives rise to Eq. (6).

$$L_p = \frac{1}{d}[(a-c)L_f + b] \tag{6}$$

A linear correlation of L_p and L_f was observed from Eq. (6). If *sign* [(a−c)/d] is negative, L_p is smaller as L_f increases. This means a cell becomes concentrated in a ball shape. On the other hand, if *sign* [(a−c)/d] is positive, L_p is larger as L_f increases. This indicates a cell becomes to spread out in a flattened shape.

Table 1. Regression analysis of R_n/L_{fr} with L_f or L_{fr}

	R_n/L_{fr} vs. L_f	R_n/L_{fr} vs. L_{fr}
Regression	$f=\frac{147.6}{x}+0.1613$	$f=\frac{0.7105}{x}-0.3061$
R^2	0.95	0.98

Peripheral length L_p is composed of L_f and L_{fix}.

$$\mathbf{L_p=L_f+L_{fix}} \tag{7}$$

Introducing Eq. (7) into Eq. (6) yields Eq. (8).

$$\mathbf{L_{fix}=\left(\frac{a-c}{d}-1\right)L_f+\frac{b}{d}} \tag{8}$$

Eq. (8) represents a linear correlation of L_f and L_{fix}. Depending on the sign of [(a−c)/d−1], the equation's meaning is totally different. If *sign* [(a−c)/d−1] is negative, L_{fix} is smaller as L_f increases. This means a cell becomes detached from its contacting cells toward segregation status when the free peripheral membrane length increases. On the other hand, if *sign* [(a−c)/d−1] is positive, L_{fix} is larger as L_f increases. This indicates a cell becomes more attached to its pre-contacting cells when the free peripheral membrane length increases.

Parameters of Eq. (4) and (5) were estimated by fitting the experimental data in Fig. 4, respectively (Table 1). Applying parameters to Eq. (8), we could get negative correlation of L_{fix} with L_f. The fitting curve is Eq. (9).

$$\mathbf{L_{fix}=-0.3422L_f+207.7\Leftrightarrow L_p=0.6578L_f+207.7} \tag{9}$$

Referring to Eq. (9), cells were proven to incline to spread out away from their surrounding cells at the expense of decreasing L_{fix}, as their free peripheral membrane length increases. L_p is the same as L_{fix} and its value is 202.8 μm as a cell is completely enclosed by its neighboring cells (L_f=0), but it is same as L_f (607.7 μm) if a cell is completely free from its neighboring cells. This can give remarkable insights into embryonic stem cells' morphological behavior when they grow and become adherent to extracellular matrix-coated surfaces. Stem cells tend to grow in a form of colony but none of the previous studies have shown mathematically how ESCs' colonial population behaves even though the movement of the cells is highly active for a long culture period. In the present system, Eq. (9) tells us that outermost cells centered on an ESC colony tend to spread out at the expense of L_{fix}, while attached to their pre-attached cells of the colony, as their free peripheral membrane moves actively. This model is meaningful to quantitatively and qualitatively demonstrate this fact and explains how an ESC colony behaves for a long-term culture period.

ACKNOWLEDGEMENTS

This research was supported by grants from Marine Biotechnology Program funded by the Ministry of Land, Transport and Maritime Affairs, Korea and from Basic Science Research Program through the National Research Foundation of Korea (**NRF**) funded by the Ministry of Education, Science and Technology (2010-0023490).

REFERENCES

1. J. S. Odorico, D. S. Kaufman and J. A. Thomson, *Stem Cells*, **19**, 193 (2001).
2. T. O'Brien and F. P. Barry, Mayo, *Clin. Proc.*, **84**, 859 (2009).
3. W. J. Fong, H. L. Tan, A. Choo and S. K. W. Oh, *Bioproc. Biosyst. Eng.*, **27**, 1615 (2005).
4. D. E. Ingber, *Biol. Bull.*, **194**, 323 (1998).
5. H. Tsuboi, J. Ando, R. Korenaga, Y. Takada and A. Kamiya, *Biochem. Biophys. Res. Commun.*, **206**, 988 (1995).
6. J. N. Topper, J. Cai, D. Falb and M. A. Gimbrone, *Proc. Natl. Acad. Sci. USA*, **93**, 10417 (1996).
7. H. J. Hsieh, N. Q. Li and J. A. Frangos, *Am. J. Physiol.*, **260**, H642 (1991).
8. I. Rivilis, M. Milkiewicz, P. Boyd, J. Goldstein, M. D. Brown, S. Egginton, F. M. Hansen, O. Hudlicka and T. L. Haas, *Am. J. Physiol. Heart Circ. Physiol.*, **283**, H1430 (2002).
9. S. Nonaka, H. Shiratori, Y. Saijoh and H. Hamada, *Nature*, **418**, 96 (2002).
10. Y. Kimiko, S. Takaaki, W. Tetsuro, M. Kohei, K. Y. Jun, O. Syotaro, O. Norihiko, M. Akiko, K. Akira and A. Joji, *Am. J. Physiol. Heart Circ. Physiol.*, **288**, H1915 (2005).
11. Y. Xia and G. M. Whitesides, *Annu. Rev. Mater. Sci.*, **28**, 153 (1998).
12. A. M. Taylor, S. W. Rhee, C. H. Tu, D. H. Cribbs, C. W. Cotman and N. L. Jeon, *Langmuir*, **19**, 1551 (2003).
13. H. S. Shin, H. J. Kim, S. K. Min, S. H. Kim, B. M. Lee and N. L. Jeon, *Biotechnol. Lett.*, **32**, 1063 (2010).
14. M. H. Kim, M. Kino-oka, M. Kawase, K. Yagi and M. Taya, *J. Biosci. Bioeng.*, **103**, 192 (2007).